Energy &
Environment Nexus

Open Access

https://doi.org/10.48130/een-0025-0007

Rapid Report

# Rational design of porphyrin-based ionophores for enhanced perchlorate selectivity in ion selective electrodes: application to fireworks wastewater analysis

Baichun Li[1], Bing Li[1], Yuze Han[1], Qimeng Li[2], Chengkui Liang[1], Shuo Zhang[1] and Wentao Li[1*]

Received: 30 June 2025

Revised: 21 July 2025

Accepted: 22 August 2025

Published online: 20 October 2025

## Abstract

The high-concentration perchlorate ($ClO_4^-$) wastewater discharged by the firework and firecracker industry poses a significant threat to the ecological security of the receiving water bodies and drinking water sources. In the context of the Internet of Things (IoT), monitoring high-concentration perchlorate wastewater necessitates intelligent control and management. This study introduces a liquid-contact ion-selective electrode (ISE) featuring novel porphyrin-based ionophores for the rapid, sensitive, and selective determination of perchlorate determination. The electrode features a poly(vinyl chloride) (PVC)-based membrane, typically called an ion-selective membrane (ISM), optimized with iron(III) *meso*-tetraphenylporphine chloride (Fe[III]TPPCl) as the ionophore, *ortho*-nitrophenyloctyl ether (NPOE) as the plasticizer, and tridodecylmethylammonium chloride (TDMACl) as the ionic additive. Systematic screening revealed Fe(III)TPPCl's superior performance over other metalloporphyrins, exhibiting a near-Nernstian slope (–68.42 ± 0.91 mV·decade$^{-1}$), a low detection limit (LOD = $10^{-5}$ M), and strong anti-interference capability, particularly against sulfate ($\log K_{ij}^{SSM}$ = –4.45). Optimization of membrane composition (1.1 wt% Fe[III]TPPCl, 65.6 wt% NPOE, 32.8 wt% PVC, 0.5 wt% TDMACl) enabled a wide linear range ($10^{-5}$–$10^{-1}$ M), fast response time (< 5 s), and stability across pH 2–10. The ISE was validated for real-sample analysis, achieving a mean recovery of 104.3% in spiked surface water and 96.4% in firework wastewater without pretreatment. Results correlated well with ion chromatography, confirming the electrode's accuracy. This work demonstrates a cost-effective, field-deployable sensor for $ClO_4^-$ monitoring in complex environmental matrices, addressing critical regulatory compliance needs.

**Keywords:** Ion-selective electrode, Perchlorate, Firework wastewater, Iron(III) *meso*-tetraphenylporphine chloride, Online monitoring

## Highlights

- Porphyrin-based derivatives with diverse substituents and coordinated metal ions were evaluated as $ClO_4^-$ ionophores.
- The optimized ISM composition consists of 1.1 wt% Fe(III)TPPCl, 65.6 wt% NPOE, 32.8 wt% PVC, and 0.5 wt% TDMACl.
- The proposed ISE exhibits a high response slope, low LOD, excellent selectivity, and a wide linear detection range.
- Rapid response (< 5 s) and broad pH stability (2–10) enable robust perchlorate detection in diverse environments.
- The ISE shows high accuracy in sample analysis, making it suitable for monitoring perchlorate in fireworks wastewater.

* Correspondence: Wentao Li (liwentao@nju.edu.cn)

Full list of author information is available at the end of the article.

## Graphical abstract

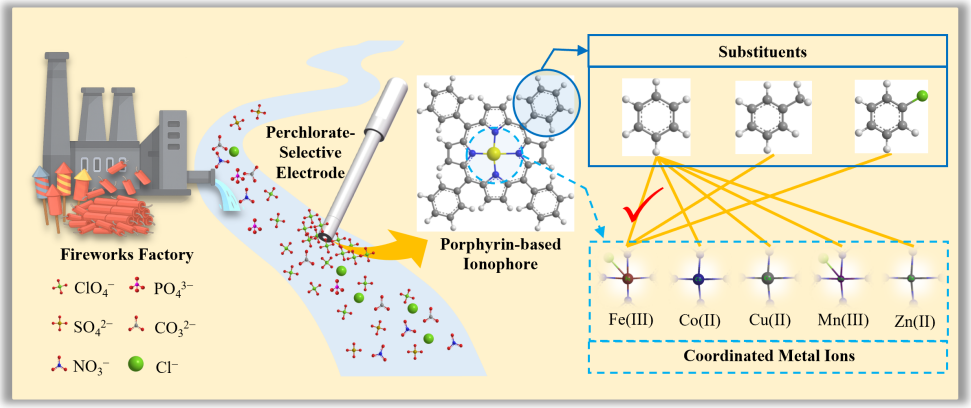


# Introduction

Perchlorate ($ClO_4^-$) is an inorganic ion that persists in the environment with origins of both natural and anthropogenic sources, and the latter prevalently originates from unintended leakage during extensive applications in industries including military defense, aerospace, manufacturing, and firework production[1–3]. It can easily contaminate surface water and groundwater, due to its high-water solubility, mobility, and stability[4,5]. For instance, the extensive production of fireworks, particularly in regions such as the Xiangjiang River Basin (China), generates considerable industrial wastewater characterized by extremely high concentrations of perchlorate (usually exceeding 1,000 mg·$L^{-1}$), and poses a considerable threat to downstream aquatic ecosystems and drinking water sources[6,7]. Although perchlorate is readily excreted by organisms, it is considered to be a health hazard due to its adverse effects on mammalian thyroid gland function, which blocks iodide uptake and reduces the secretion of thyroid hormones[8–10]. In response to these concerns, the WHO Guidelines for Drinking-Water Quality and China's Latest National Standard for Drinking Water GB 5749-2022 explicitly established a maximum allowable concentration of 70 μg·$L^{-1}$ for perchlorate in drinking water. Thus, effective and frequent detection is critical for mitigating the environmental and health impacts of this pollutant.

Various analytical techniques have been employed for perchlorate determination, including gravimetry, atomic absorption spectrometry (AAS), ion chromatography (IC), liquid chromatography-tandem mass spectrometry (LC-MS/MS), and electrochemical sensing methods such as ion-selective electrodes (ISEs)[11–15]. Among these, ISEs stand out for their promising alternative for portable or on-site continuous monitoring, with benefits of low cost, high reliability and validity, and ease of operation[16,17]. Structurally, ISEs can be categorized into liquid-contact (with an internal filling solution), and solid-contact (featuring an ion-to-electron transducer) configurations[18]. Regardless of the configuration, their core performance characteristics—sensitivity (slope), detection limit (LOD), selectivity, and linear range—are primarily determined by the composition of the ion-selective membrane (ISM). The ISM is typically a complex mixture composed of a polymer matrix (e.g., PVC), a plasticizer, an ionophore (ion carrier), and often an ionic additive (ion exchanger)[19]. The ionophore is responsible for selectively extracting target ions from the sample interface into the ISM. Therefore, ionophores typically possess functional groups capable of accommodating multiple target ions or structures with coordination spaces and specific binding sites that enable ion-selective recognition[20].

The selectivity of traditional ionophores, such as lipophilic quaternary ammonium salts, for various anions generally follows the Hofmeister series[21], as their electrostatic interactions with target anions govern the observed potential responses. This trend, for anions, is typically observed as: $ClO_4^-$ > $SCN^-$ > $I^-$ > salicylate > $NO_3^-$ > $Br^-$ > $NO_2^-$ > $Cl^-$ > $HSO_3^-$ > acetate > $SO_4^{2-}$ > $HPO_4^{2-}$. Ionophore selectivity can be enhanced and tailored during synthesis to render the ligand site more sterically compatible with perchlorate ions[22]. Numerous studies have evaluated the application of newly synthesized ionophores derived from various structures, including calix(4)arenes[23–26], metal complexes (Ni[27–29], Pt[30,31], Co[32,33], Cu[34,35], Zn[36], Au[37], etc.) porphyrins[38,39] and other supramolecular architectures[40–44]. Metalloporphyrin-based anion-selective electrodes frequently demonstrate anti-Hofmeister selectivity. Porphyrins and their metal complexes offer notable advantages as molecular recognition elements: they exist in diverse structural forms, feature a rigid molecular scaffold, allow precise control over ring substituent positioning, and enable modulation of both the steric environment around the axial coordination site and interaction directionality via variation of the central metal ion[45]. Therefore, further investigation is warranted into how substituent structures at specific ring positions influence the hydrophilic/hydrophobic properties of porphyrins, as well as the role of different coordinated metal ions.

In this study, a plasticized PVC membrane perchlorate-selective liquid electrode was developed, utilizing metal-based porphyrin derivatives as ionophores. This electrode offers a wide linear dynamic range and robust anti-interference capability, making it suitable for simple and rapid perchlorate determination. The developed electrode has been successfully used for the direct measurement of wastewater from fireworks and surface water, eliminating the need for pretreatment of the water samples.

# Materials and methods

## Reagents and materials

Unless otherwise noted, reagent grade chemicals were purchased and used as received. The chemical reagents used as ionophores included the following metalloporphyrins: iron(III) *meso*-tetraphenylporphine chloride (Fe[III]TPPCl), iron(III) 5,10,15,20-tetrakis(4-methylphenyl)

porphyrin chloride (Fe[III]TMPPCl), iron(III) 5,10,15,20-tetrakis(4-chlorophenyl)porphyrin chloride (Fe[III]TClPPCl), cobalt(II) tetraphenylporphyrin (Co[II]TPP), copper(II) tetraphenylporphyrin (Cu[II]TPP), manganese(III) *meso*-tetraphenylporphine chloride (Mn[III]TPPCl), and zinc(II) tetraphenylporphyrin (Zn[II]TPP). The following ion-pair agents were employed as the ionic additives, including hexadecyl trimethyl ammonium bromide (CTAB), tridodecylmethylammonium chloride (TDMACl), and methyltrioctylammonium chloride (MTOACl). The reagents used as plasticizers were bis(2-ethylhexyl) sebacate (DOS), Dibutyl phthalate (DBP), Dioctylphthalate (DOP), and *ortho*-nitrophenyloctyl ether (NPOE), and the polymer matrix was selected as high molecular weight Poly(vinyl chloride) (PVC). These chemicals are listed in Supplementary Table S1, along with chemical structure and CAS number.

Stock solutions (1 M) of $ClO_4^-$ and interfering anions (e.g., $PO_4^{3-}$, $SO_4^{2-}$, $CO_3^{2-}$, $NO_3^-$, $Cl^-$) were prepared in deionized water (≥ 18 MΩ·cm), and working solutions were obtained by serial dilution as needed.

## ISE preparation and optimization

The ISMs were prepared by dissolving specific amounts of PVC, plasticizer, ionophore, and ionic additive in 5 mL of tetrahydrofuran (THF). The homogeneous solution was poured into a glass culture dish (diameter ~35 mm), and covered loosely to allow THF evaporation overnight in an electric thermostatic drying oven, resulting in a smooth elastic membrane with thickness of ~0.8 mm. Small disks ($\varphi$ ~7 mm) were punched using a hole puncher from the master membrane.

As designed in Supplementary Fig. S1, the ISE body was machined using a polyoxymethylene tube with an outer diameter of ~12 mm. A small disk of the prepared ISM was fixed to one end with a cap, and an Ag/AgCl wire was inserted and sealed in the other end. The ISE was filled with solution ($10^{-2}$ M $NaClO_4 \cdot H_2O$), and conditioned in $10^{-2}$ M $NaClO_4 \cdot H_2O$ solution for at least 24 h before use.

The experiments for the screening of ionophores, ionic additives, and plasticizers and the optimization of their composition are listed in Table 1**.** Key performance parameters, including linearity, sensitivity, and selectivity, were determined.

## Electromotive Force (EMF) measurements and ISE evaluation

All EMF measurements of ISEs were performed at room temperature (25 ± 1 °C) using a high-impedance digital mV meter/pH meter (Model PHSJ-6L, Leici, China) with an Ag/AgCl reference electrode (Model 216, Xianfeng, China). The EMF measurement of the ISE electrode was conducted with the working solutions of $ClO_4^-$ concentration ranging from $10^{-7}$ to $10^{-1}$ M. When measuring, the working solution or water sample was magnetically stirred, and the potentiometric response was record after stabilization. The slope (mV·decade$^{-1}$) and linear range were calculated from the calibration curve (E vs logc[$ClO_4^-$]), and the practical LOD was determined as the intersection of the extrapolated linear segments of the calibration curve.

The selectivity coefficients were determined using the separate solution method (SSM). Initially, potential responses were measured in the target ion solution, and $E_i^0$ was calculated by extrapolating

**Table 1** Optimization of PVC-based membrane sensors with varied plasticizers and ionophores: comparative evaluation of sensitivity, linearity, and selectivity for metal-based porphyrin derivatives detection

| Category | Ionophores | Plasticizers | Ionic additives | PVC / plasticizers / ionophores / ionic additives (mg)[a] | Evaluation test |
|---|---|---|---|---|---|
| I | Fe(III)TPPCl | NPOE | CTAB | 600 :1200 : 20 : 60 | Linearity, Sensitivity and Selectivity Coefficient |
| | Fe(III)TMPPCl | | | 600 : 1200 : 20 : 60 | |
| | Fe(III)TClPPCl | | | 600 : 1200 : 20 : 60 | |
| | Co(II)TPP | | | 600 : 1200 : 20 : 60 | |
| | Cu(II)TPP | | | 600 : 1200 : 20 : 60 | |
| | Mn(III)TPPCl | | | 600 : 1200 : 20 : 60 | |
| | Zn(II)TPP | | | 600 : 1200 : 20 : 60 | |
| II | Fe(III)TPPCl | DOS | CTAB | 600 : 600 : 20 : 60 | Linearity and Sensitivity |
| | | | | 600 : 900 : 20 : 60 | |
| | | | | 600 : 1200 : 20 : 60 | |
| | | | | 600 : 1500 : 20 : 60 | |
| | | DOP | | 600 : 600 : 20 : 60 | |
| | | | | 600 : 900 : 20 : 60 | |
| | | | | 600 : 1200 : 20 : 60 | |
| | | | | 600 : 1500 : 20 : 60 | |
| | | DBP | | 600 : 600 : 20 : 60 | |
| | | | | 600 : 900 : 20 : 60 | |
| | | | | 600 : 1200 : 20 : 60 | |
| | | | | 600 : 1500 : 20 : 60 | |
| | | NPOE | | 600 : 600 : 20 : 60 | |
| | | | | 600 : 900 : 20 : 60 | |
| | | | | 600 : 1200 : 20 : 60 | |
| | | | | 600 : 1500 : 20 : 60 | |
| III | Fe(III)TPPCl | NPOE | TDMACl | 600 : 1200 : 20 : 10 | Linearity, Sensitivity and Selectivity Coefficient |
| | | | | 600 : 1200 : 20 : 20 | |
| | | | | 600 : 1200 : 20 : 40 | |
| | | | CTAB | 600 : 1200 : 20 : 10 | |
| | | | | 600 : 1200 : 20 : 20 | |
| | | | | 600 : 1200 : 20 : 40 | |
| | | | MTOACl | 600 : 1200 : 20 : 10 | |
| | | | | 600 : 1200 : 20 : 20 | |
| | | | | 600 : 1200 : 20 : 40 | |

[a] Add the components to 5 mL of THF in the listed proportions.

the response to $a_i$ = 1 M. Subsequently, potentiometric responses were measured for various interfering ions. $E_j^0$ was determined using the same procedure. Finally, the selectivity coefficients ($K_{ij}$, where $i$ is the target ion, and $j$ is the interfering ion) were calculated using the potential at 1 M based on the Nicolsky-Eisenman equation[46]:

$$K_{ij} = \exp\left\{\frac{E_j^0 - E_i^0}{RT} z_i F\right\} \quad (1)$$

where, $z_i$ is the charge of the target ion. $R$, $T$, and $F$ denote the gas constant, the absolute temperature, and the Faraday constant, respectively.

The dynamic response time is a critical performance parameter for perchlorate-selective electrodes, as it determines the electrode's applicability for real-time monitoring scenarios[47]. In this study, the response behavior of the optimized Fe(III)TPPCl-based electrode was evaluated under stepwise increases in $ClO_4^-$ concentration, ranging from 1.0 × $10^{-5}$ to 1.0 × $10^{-1}$ M. The pH of the sample solution is a critical factor that can significantly influence the response of the ISE. Thus, the influence of pH was investigated by recording the potential of $10^{-4}$ M to $10^{-1}$ M $ClO_4^-$ solutions while adjusting the pH from 2 to 10 using incremental additions of 1 M $H_2SO_4$ or NaOH.

The prepared ISE was finally applied to 15 surface water and five firework manufacturing wastewaters, which were spiked with 100 and 200 mg·$L^{-1}$ of $ClO_4^-$, respectively.

# Results and discussion

## Screening of ISM ionophores for $ClO_4^-$

The selection of suitable ionophores is fundamental to the design of ISEs, as it directly determines their selectivity, sensitivity, and detection performance toward target ions[48]. To ensure consistency across formulations, all membranes were fabricated using a fixed composition of PVC (32 wt%, 600 mg), plasticizer (NPOE, 64 wt%, 1,200 mg), CTAB,

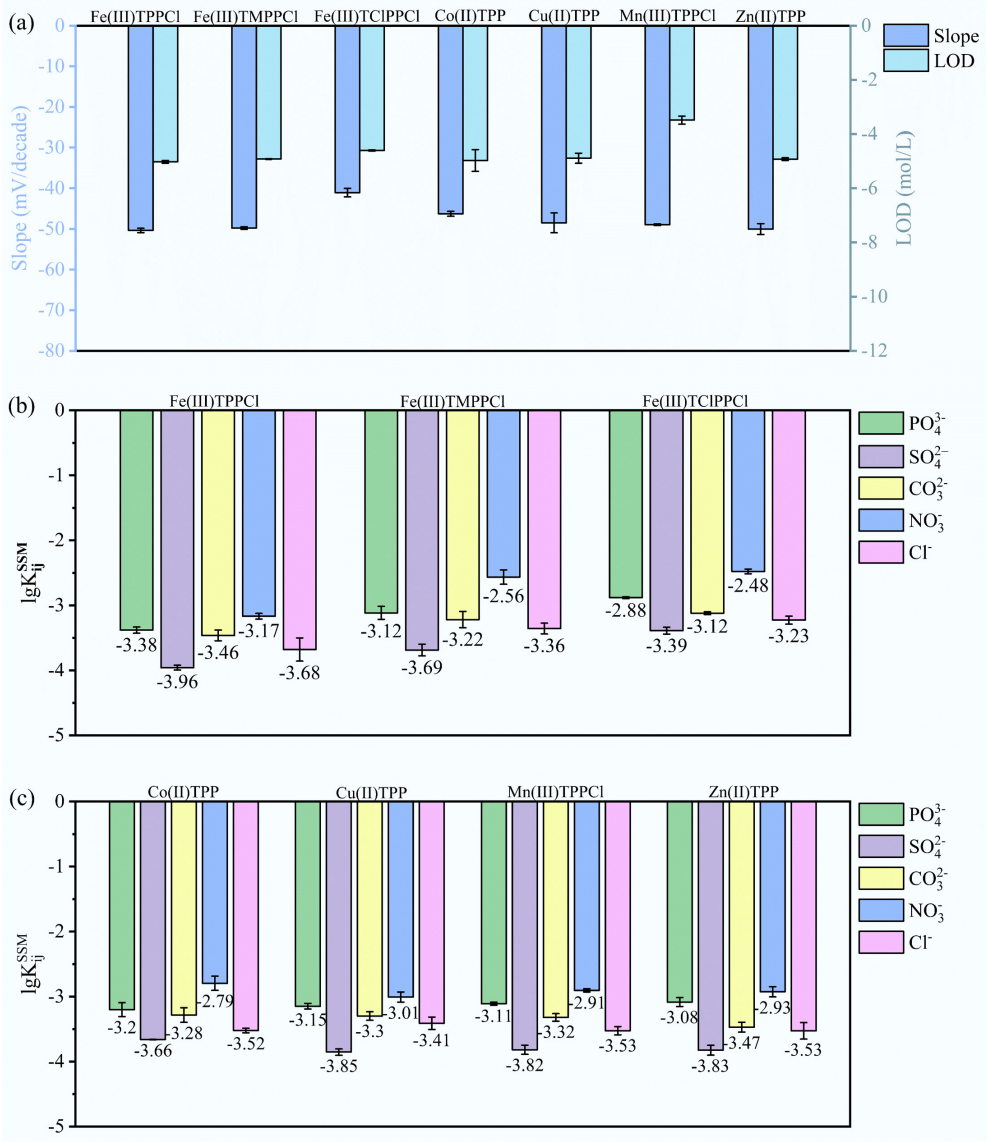


**Fig. 1** Response slopes, detection limits, and selectivity coefficients for porphyrin-based ionophores. (**a**) Response slopes (left axis) and detection limits (right axis). (**b**) Selectivity coefficients $logK_{ij}^{SSM}$ of porphyrin-based ionophores with different substituents. (**c**) Selectivity coefficients $logK_{ij}^{SSM}$ of porphyrin-based ionophores with different coordinated metal ions.

and candidate ionophore at a 3:1 weight ratio. The performances of ISEs using these porphyrin-based ionophores were systematically compared based on three key parameters, including response slope, LOD, and selectivity toward $ClO_4^-$ vs common interfering anions (Fig. 1, Supplementary Table S2).

As shown in Fig. 1a, the left and right axes represent the response slope and LOD of ISEs, respectively. Among the porphyrin-based ionophores with different substituent structures, Fe(III)TPPCl exhibited the most favorable response, with a response slope −50.37 ± 0.56 mV·decade$^{-1}$. In contrast, Fe(III)TClPPCl exhibited a comparatively lower slope (−41.08 ± 1.05 mV·decade$^{-1}$), suggesting suboptimal ion recognition. Thus, the porphyrin substituted with electron-withdrawing group would decrease the response slope of ISE. For the porphyrin-based ionophores with different coordinated metal ions, Fe(III)TPPCl, Cu(II)TPP, and Zn(II)TPP exhibited comparable response slope with LODs reached ~$10^{-5}$ M; while the Co(II)TPP showed an observable lower response slope (−46.29 ± 0.62 mV·decade$^{-1}$), and Mn(III)TPPCl exhibited a poor LOD of ~$10^{-3.5}$ M.

Figure 1b, c compared the logarithmic selectivity coefficients ($\log K_{ij}^{SSM}$) of ISEs, using porphyrin-based ionophores with different substituent groups and different coordinated metal ions, against a range of interfering anions including $PO_4^{3-}$, $SO_4^{2-}$, $CO_3^{2-}$, $NO_3^-$, and $Cl^-$. In general, the selectivity of all the ISEs against interfering ions followed the order as follows: $SO_4^{2-} > Cl^- > CO_3^{2-} > PO_4^{3-} > NO_3^-$. Among porphyrin-based ionophores with different porphyrin ring structures, the Fe(III)TPPCl exhibited the strongest selectivity, particularly against $SO_4^{2-}$ ($\log K_{ij}^{SSM} = -3.96$), indicating a strong preference for sulfate over other competing anions, while the Fe(III)TClPPCl showed the lowest selectivity; its porphyrin ring is substituted with electron-withdrawing group. Among the test coordinated metal ions, the selectivity slightly decreased in the order of Fe(III)TPPCl > Cu(II)TPP > Zn(II)TPP > Mn(III)TPPCl > Co(II)TPP. The superior performance of Fe(III)TPPCl toward $ClO_4^-$ is attributed to the preferential axial coordination between Fe(III), a hard Lewis acid, and $ClO_4^-$, which is classified as a hard Lewis base due to its high electronegativity, low polarizability, and strongly hydrated tetrahedral structure composed of oxygen atoms[49–51]. This hard-hard acid-base pairing favors specific electrostatic interactions, contributing to selective perchlorate recognition over softer or more polarizable anions. Additionally, the binding constant of this perchlorate interaction is significantly higher than that of most other anions.

Consequently, Fe(III)TPPCl was screened as the most effective ionophore towards $ClO_4^-$, offering the optimal combination of sensitivity, low LOD, and high selectivity. However, its slope did not reach the theoretical Nernstian value of −59 mV·decade$^{-1}$, and thus further optimization of ISM composition is required to enhance its overall electrode performance in practical applications.

## Selection and optimization of ISM plasticizer

Plasticizers, such as DOS, DOP, DBP, and NPOE, are incorporated into ISMs to enhance mechanical flexibility, facilitate ion mobility, and regulate membrane dielectric properties. Selecting a plasticizer with appropriate polarity ensures compatibility with the ionophore and further promotes enhanced selectivity and sensitivity of the membrane[20,52]. As shown in Table 2 and Supplementary Table S3, a variety of plasticizer types and loadings were tested for the ISMs with the constant amounts of polymer matrix, ionophore, and ionic additives (i.e., 600 mg PVC, 20 mg Fe[III]TPPCl, and 60 mg CTAB). With increasing plasticizer proportion, the performance of ISMs in terms of linear range and LOD initially demonstrated enhancement, followed by marginal performance deterioration. Consistent with previous literature[53], the optimal ratio of plasticizer to PVC is 2:1–2.5:1. Under this proportional condition, the ISM using NPOE achieved a slope of −44.03 mV·decade$^{-1}$, an extended linear range from $10^{-7}$ to $10^{-1}$ M, and a remarkably LOD of $10^{-6.53}$ M, which is below the WHO limit and median LOD of the reported ISEs[22]. This is attributed to NPOE's high dielectric constant (~23.1), which promotes ion migration and improves the ion-exchange equilibrium at the membrane interface[54]. For the other plasticizers, the corresponding detection limits ranged from $10^{-5.04}$ to $10^{-5.1}$ M. Additionally, the response slopes of the ISMs were observed in an order of NPOE > DBP > DOS > DOP.

Thus, the plasticizer and polymer matrix composition for ISM based on Fe(III)TPPCl ionophore was optimized as NPOE at a 2:1 ratio to PVC.

## Selection and optimization of ISM ionic additive

Ionic additives play a crucial role in ion-selective membranes by facilitating specific ion transport while excluding interferents. They also neutralize the charge of the ionophore-analyte complex, thereby enhancing membrane conductivity and enabling efficient ion exchange[55]. Figure 2 and Supplementary Table S4 systematically compare the effect of ionic additives on the sensitivity, LOD, and

**Table 2** Composition of membranes and potentiometric response characteristics of perchlorate-selective electrodes based on Fe(III)TPPCl

| No. | Composition (mg) | | | | Slope (mV·decade$^{-1}$) | Linear range (M) | LOD (M) |
|---|---|---|---|---|---|---|---|
| | PVC | Plasticizers | Ionophores | Ionic additives | | | |
| 1 | 600 | DOS, 600 | Fe(III)TPPCl, 20 | CTAB, 60 | −46.33 | $10^{-4}$ ~ $10^{-1}$ | $10^{-4.07}$ |
| | | DOS, 900 | | | −39.89 | $10^{-5}$ ~ $10^{-1}$ | $10^{-5.17}$ |
| | | DOS, 1200 | | | −47.78 | $10^{-5}$ ~ $10^{-1}$ | $10^{-5.07}$ |
| | | DOS, 1500 | | | −40.48 | $10^{-5}$ ~ $10^{-1}$ | $10^{-4.95}$ |
| 2 | 600 | DOP, 600 | Fe(III)TPPCl, 20 | CTAB, 60 | −31.65 | $10^{-4}$ ~ $10^{-1}$ | $10^{-3.99}$ |
| | | DOP, 900 | | | −35.48 | $10^{-4}$ ~ $10^{-1}$ | $10^{-3.9}$ |
| | | DOP, 1200 | | | −39.05 | $10^{-5}$ ~ $10^{-1}$ | $10^{-5.04}$ |
| | | DOP, 1500 | | | −35.15 | $10^{-5}$ ~ $10^{-1}$ | $10^{-4.95}$ |
| 3 | 600 | DBP, 600 | Fe(III)TPPCl, 20 | CTAB, 60 | −40.66 | $10^{-4}$ ~ $10^{-1}$ | $10^{-4.01}$ |
| | | DBP, 900 | | | −43.09 | $10^{-5}$ ~ $10^{-1}$ | $10^{-5.21}$ |
| | | DBP, 1200 | | | −50.83 | $10^{-5}$ ~ $10^{-1}$ | $10^{-4.99}$ |
| | | DBP, 1500 | | | −55.09 | $10^{-5}$ ~ $10^{-1}$ | $10^{-5.1}$ |
| 4 | 600 | NPOE, 600 | Fe(III)TPPCl, 20 | CTAB, 60 | −50.92 | $10^{-3}$ ~ $10^{-1}$ | $10^{-3.17}$ |
| | | NPOE, 900 | | | −57.08 | $10^{-3}$ ~ $10^{-1}$ | $10^{-3.47}$ |
| | | NPOE, 1200 | | | −44.03 | $10^{-7}$/$10^{-6}$ ~ $10^{-1}$ | $10^{-6.53}$ |
| | | NPOE, 1500 | | | −59.19 | $10^{-4}$ ~ $10^{-1}$ | $10^{-4.3}$ |

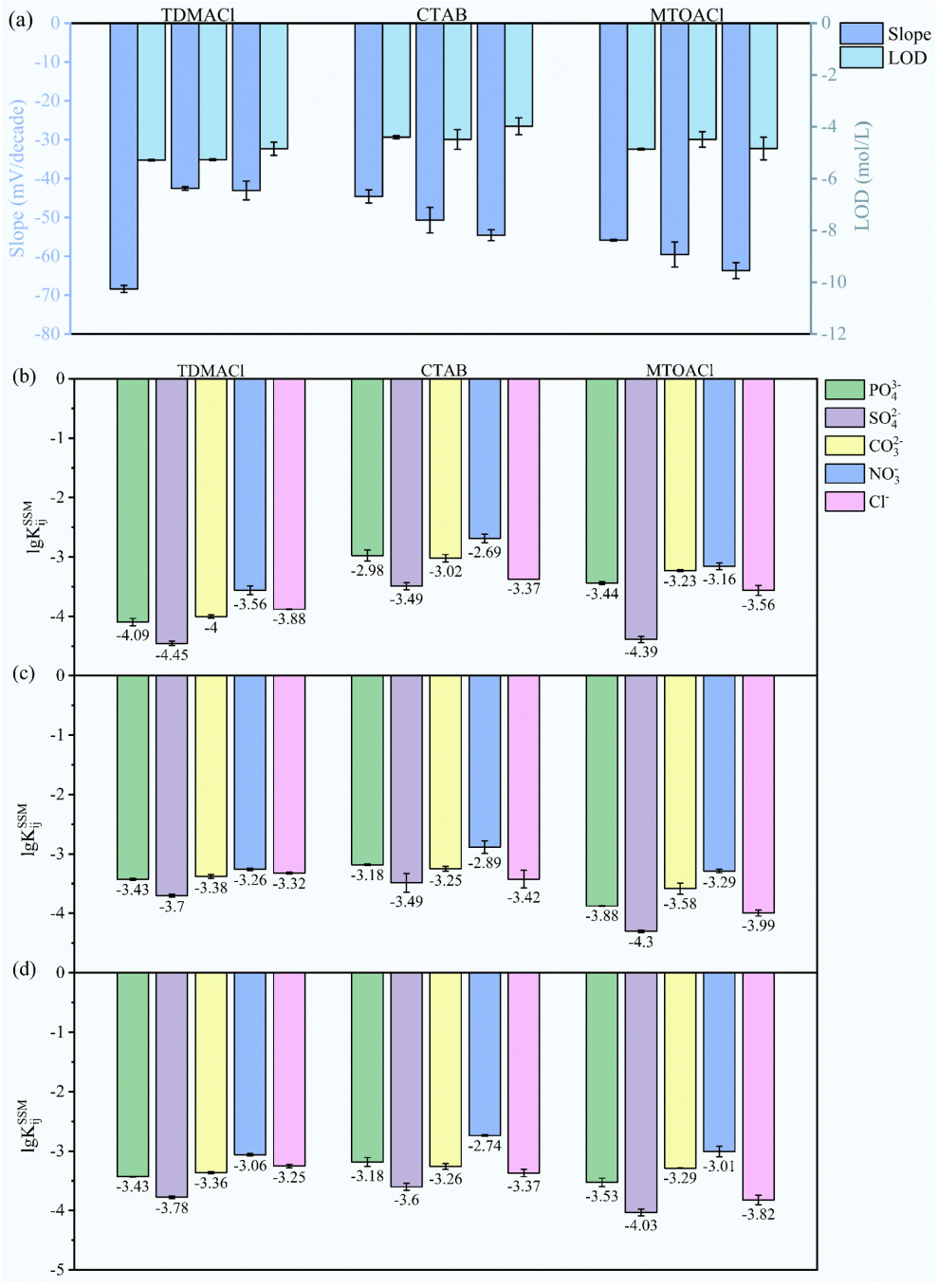


**Fig. 2** Response slopes, detection limits, and selectivity coefficients for ionic additives at varying additive-to-ionophore ratios. (**a**) Response slopes (left axis) and detection limits (right axis) of various ionic additives at 1:2, 1:1, 2:1 additive-to-ionophore ratios. (**b**) Selectivity coefficients $logK_{ij}^{SSM}$ of ionic additives at a 1:2 additive-to-ionophore ratio against various interfering ions. (**c**) Selectivity coefficients $logK_{ij}^{SSM}$ of ionic additives at a 1:1 additive-to-ionophore ratio against various interfering ions. (**d**) Selectivity coefficients $logK_{ij}^{SSM}$ of ionic additives at a 2:1 additive-to-ionophore ratio against various interfering ions.

selectivity of ISMs, which were fabricated using the optimal ionophore Fe(III)TPPCl and plasticizer NPOE (NPOE : PVC = 2:1), while varying the type and concentration of ionic additives (TDMACl, CTAB, MTOACl) at weight ratios of 1:2, 1:1, and 2:1 relative to the ionophore.

As shown in Fig. 2a, the left Y-axis indicates the slope (mV·decade$^{-1}$) of the electrode response to $ClO_4^-$ under various ionic additive conditions. Among all tested formulations, the membrane containing TDMACl at a 1:2 ratio to Fe(III)TPPCl exhibited the highest sensitivity with a slope of –68.42 ± 0.91 mV·decade$^{-1}$, exceeding the theoretical Nernstian value, suggesting the addition of specific amounts of ionic additives enhances the sensitivity of the electrode. For TDMACl, increasing its proportion beyond the 1:2 ratio led to reduced slopes, suggesting that excess TDMACl compromises membrane performance. In contrast, CTAB and MTOACl showed increasing slopes with additive concentration, with MTOACl reaching near-Nernstian performance at –59.71 ± 3.89 mV·decade$^{-1}$, whereas CTAB remained suboptimal in sensitivity, with response slopes below the theoretical Nernstian value. The right Y-axis in

Fig. 2a illustrates the LODs, with lower values indicating higher sensitivity. Both TDMACl and MTOACl achieved low LODs around $10^{-5}$ M, highlighting their superior detection capabilities. In contrast, CTAB resulted in relatively poorer LODs, suggesting less favorable ion exchange efficiency and membrane conductivity.

Figure 2b–d further presents the selectivity of ISM to $ClO_4^-$, against interfering anions $PO_4^{3-}$, $SO_4^{2-}$, $CO_3^{2-}$, $NO_3^-$, and $Cl^-$. Notably, the TDMACl : Fe(III)TPPCl = 1:2 configuration yielded the most favorable selectivity profile, with $\log K_{ij}^{SSM}$ values lower than –4 against $SO_4^{2-}$, $PO_4^{3-}$, and $CO_3^{2-}$. The selectivity coefficients obtained for the proposed electrode showed a selectivity sequence of anions in the following order: $SO_4^{2-} > PO_4^{3-} > CO_3^{2-} > Cl^- > NO_3^-$. This superior performance is likely attributed to the high lipophilicity of TDMACl, which enhances membrane conductivity, facilitates rapid ion exchange, and improves $ClO_4^-$ affinity while reducing resistance and interference. Moreover, lipophilic additives promote phase homogeneity and prevent ion-pair formation with interfering anions, thereby increasing the selectivity and stability of the membrane[34,56]. The final optimized membrane composition was determined to be: Fe(III)TPPCl (1.1 wt%), NPOE (65.6 wt%), PVC (32.8 wt%), and TDMACl (0.5 wt%).

## Performances of the optimized ISE

The dynamic response time is a critical performance parameter for ISE, as it determines the electrode's applicability for real-time monitoring scenarios. Figure 3a presents the time-resolved potential response of the optimized ISE upon successive $ClO_4^-$ concentration steps from $1.0 \times 10^{-5}$ to $1.0 \times 10^{-1}$ M. Notably, the electrode achieved a stable potential within approximately 5 s after each concentration change, confirming its rapid response characteristics. The clear and stable plateaus corresponding to each concentration level indicated a well-defined Nernstian behavior. The optimized ISE also showed a wide linear range from $10^{-5}$ to $10^{-1}$ M with a slope of –66.63 ± 1.29 mV·decade$^{-1}$ and a coefficient of determination $R^2 = 0.999$, as shown in the inset. For detailed data, refer to Supplementary Table S5. The electrode stability test was conducted in a $10^{-4}$ M $NaClO_4{\cdot}H_2O$ solution over a continuous 5-h period. The potential fluctuated within a narrow range of 297 to 305 mV, indicating good short-term stability. For detailed data, refer to Supplementary Table S6 and Supplementary Fig. S2.

Figure 3b depicts the pH dependence of the optimized ISE over the pH range from 2 to 10 at a constant $ClO_4^-$ concentration of $10^{-4}$, $10^{-3}$, $10^{-2}$, and $10^{-1}$ M, respectively. The potentiometric response of ISE remained relatively stable at an acidic pH no matter of the $ClO_4^-$ concentration, suggesting that the competitive protonation or deprotonation of the ion carrier or plasticizer was not significantly affected[57,58]. The potentiometric response slightly increased when pH increased to ~10, which is possibly due to interference of hydroxide ions for $ClO_4^-$ exchange sites on the membrane. Despite being slightly affected by alkaline pH, the optimized ISE exhibited a mean response slope of –72.22 ± 2.83 mV·decade$^{-1}$ and a $R^2$ value of 0.997 ± 0.003 across all pH conditions (Supplementary Table S7).

To validate its practical applicability, the optimized ISE was employed to quantify $ClO_4^-$ concentrations in 15 surface water and five firework manufacturing wastewater samples, which were

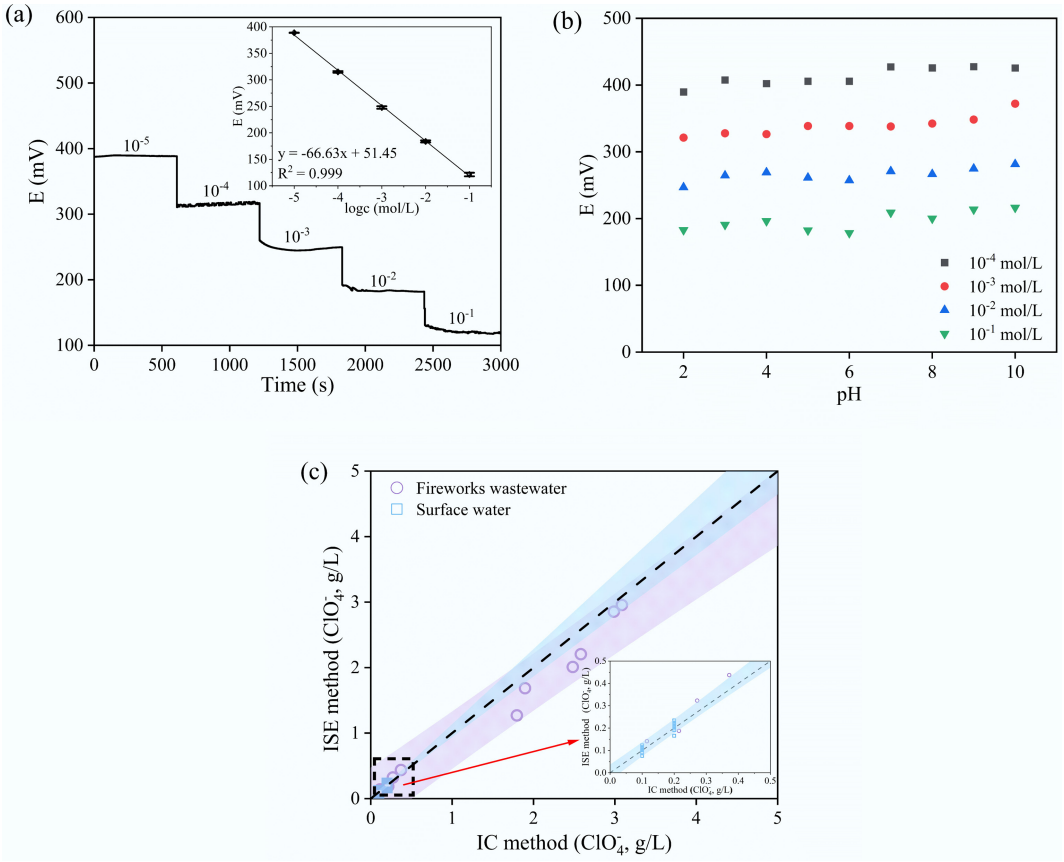


**Fig. 3** Evaluation performance of the proposed ISE. **(a)** Dynamic response time of optimal electrode for step changes in concentration of $ClO_4^-$ (low to high), inset graph represents the linear region of the average values obtained over the 2- to 10-min interval. **(b)** Effect of pH of test solutions on the response of the proposed optimized electrode: $10^{-4}$–$10^{-1}$ M $NaClO_4{\cdot}H_2O$. **(c)** Evaluation of ion-selective electrode accuracy in real wastewater samples.

further spiked with 100 and 200 mg·L$^{-1}$ $ClO_4^-$, respectively. As summarized in Supplementary Table S8, the original $ClO_4^-$ concentrations in surface water samples were negligible, and the recovery rates were in the range of 75.9%–123.1% with an average value of 104.3%; while the original $ClO_4^-$ concentrations fireworks manufacturing wastewater samples were 14.8, 171.8, 1,695.2, 2,381.9, and 2,886.5 mg·L$^{-1}$, respectively, and the recovery rates ranged from 70.8% to 122.9% with a mean value of 96.4%. As illustrated in Fig. 3c, a strong correlation was observed between perchlorate concentrations measured by the ion-selective electrode (ISE) method and ion chromatography (IC) in firework wastewater (purple circles) and surface water (blue squares). The shaded regions represent the 95% confidence intervals for each data set, and the inset highlights the low concentration range (0–500 mg·L$^{-1}$), illustrating good agreement between the two methods across different sample matrices. These findings confirm that the proposed electrode is not only selective and sensitive but also robust for *in situ* determination of perchlorate in diverse environmental water bodies.

## Conclusions

This study successfully developed and optimized a high-performance perchlorate-selective electrode based on Fe(III)TPPCl as the ionophore. Key findings include ionophore screening, which confirmed Fe(III)TPPCl's superiority over other metalloporphyrins (e.g., Co[II]TPP, Mn[III]TPPCl) and substituted analogs (e.g., Fe[III]TClPPCl), delivering optimal sensitivity (slope: –68.42 ± 0.91 mV·decade$^{-1}$), low LOD ($10^{-5}$ M), and exceptional selectivity against common anions ($SO_4^{2-}$ > $PO_4^{3-}$ > $CO_3^{2-}$ > $Cl^-$ > $NO_3^-$). The Fe(III) center's axial coordination with $ClO_4^-$ and electron-donating phenyl groups were critical in promoting anti-Hofmeister behavior. Membrane optimization identified NPOE as the ideal plasticizer (dielectric constant ~23.1) at a 2:1 ratio to PVC, extending the linear range to $10^{-5}$–$10^{-1}$ M. TDMACl enhanced sensitivity and selectivity by improving ion exchange kinetics and membrane homogeneity. Real-world applicability was demonstrated in fireworks wastewater (perchlorate: 14.8–2,886.5 mg·L$^{-1}$) and surface water. The electrode achieved quantitative recoveries (96.4% mean for wastewater and 104.3% for surface water) without the need for sample pretreatment, closely aligning with ion chromatography results. Its robustness across pH 2–10 and rapid response (< 5 s) support its field deployment. Plus, based on current raw material pricing and fabrication procedures, the estimated cost per unit for the proposed liquid-contact ISE is below USD $2 (Supplementary Table S9), making it suitable for low-cost and disposable perchlorate monitoring in industrial wastewater scenarios.

Despite its favorable performance, this study is subject to certain limitations. The current electrode design relies on a liquid-contact configuration, which may present challenges for long-term deployment due to potential leakage of the internal solution or instability under varying temperatures. Future work will focus on prolonging electrode lifespan and transitioning to solid-contact ISE configurations to improve field robustness.

## Supplementary information

It accompanies online at: https://doi.org/10.48130/een-0025-0007.

## Author contributions

All authors contributed to the study conception and design. Data collection and analysis were performed by Baichun Li, Bing Li, Chengkui Liang, and Shuo Zhang. Conceptualization and the first draft of the manuscript was written by Baichun Li, and all authors commented on previous versions of the manuscript. Funding acquisition was provided by Wentao Li, and resources were provided by Qimeng Li. Methodology development and validation were led by Yuze Han, with supervision and project administration by Wentao Li. All authors reviewed the results and approved the final version of the manuscript.

## Data availability

The datasets generated during and/or analyzed in the current study are available from the corresponding author on reasonable request.

## Funding

This work was supported by the National Key Research and Development Program of China (2022YFC3204900).

## Declarations

### Competing interests

Wentao Li is an editorial board member of *Energy & Environment Nexus* and was not involved in the editorial review or the decision to publish this article. All authors declare that there are no competing interests.

### Author details

[1]State Key Laboratory of Water Pollution Control and Green Resource Recycling, School of the Environment, Nanjing University, Nanjing 210023, China; [2]School of Environment, Jiangsu Engineering Lab of Water and Soil Eco-remediation, Nanjing Normal University, Nanjing 210023, China

### References

[1] Srinivasan R, Sorial GA. 2009. Treatment of perchlorate in drinking water: a critical review. *Separation and Purification Technology* 69:7–21

[2] Urbansky ET. 2002. Perchlorate as an environmental contaminant. *Environmental Science and Pollution Research* 9:187–192

[3] Aziz CE, Hatzinger PB. 2009. Perchlorate sources, source identification and analytical methods. In *In Situ Bioremediation of Perchlorate in Groundwater*, ed. Stroo HF, Ward CH. New York, NY: Springer. pp. 55–78 doi: 10.1007/978-0-387-84921-8_4

[4] Cao F, Jaunat J, Sturchio N, Cancès B, Morvan X, et al. 2019. Worldwide occurrence and origin of perchlorate ion in waters: A review. *Science of The Total Environment* 661:737–749

[5] Fang C, Naidu R. 2023. A review of perchlorate contamination: analysis and remediation strategies. *Chemosphere* 338:139562

[6] Zhang B, An W, Shi Y, Yang M. 2022. Perchlorate occurrence, sub-basin contribution and risk hotspots for drinking water sources in China based on industrial agglomeration method. *Environment International* 158:106995

[7] Dou D, He M, Liu J, Xiao S, Gao F, et al. 2024. Occurrence, distribution characteristics and exposure assessment of perchlorate in the environment in China. *Journal of Hazardous Materials* 474:134805

[8] Steinmaus CM. 2016. Perchlorate in water supplies: sources, exposures, and health effects. *Current Environmental Health Reports* 3:136–143

[9] Wolff J. 1998. Perchlorate and the thyroid gland. *Pharmacological Reviews* 50:89–105

[10] Leung AM, Pearce EN, Braverman LE. 2010. Perchlorate, iodine and the thyroid. *Best Practice & Research Clinical Endocrinology & Metabolism* 24:133–141

[11] Hefter G. 2018. A simple gravimetric method for the determination of perchlorate. *Monatshefte für Chemie - Chemical Monthly* 149:323–326

[12] Cyganski A, Kowalczyk P. 2000. New cetyltrimethylammoniulu methods for the determination of perchlorates. *Chemia Analityczna* 45(6):911–919

[13] Gallego M, Valcárcel M. 1985. Indirect atomic absorption spectrometric determination of perchlorate by liquid-liquid extraction in a flow-injection system. *Analytica Chimica Acta* 169:161–169

[14] Chattaraj S, De K, Das AK. 1992. Indirect determination of perchlorate by atomic absorption spectrometry. *Microchimica Acta* 106:183–190

[15] Hu J, Xian Y, Wu Y, Chen R, Dong H, et al. 2021. Perchlorate occurrence in foodstuffs and water: Analytical methods and techniques for removal from water – a review. *Food Chemistry* 360:130146

[16] Zuliani C, Diamond D. 2012. Opportunities and challenges of using ion-selective electrodes in environmental monitoring and wearable sensors. *Electrochimica Acta* 84:29–34

[17] Polidori G, Tonello S, Serpelloni M. 2024. Ion-selective all-solid-state printed sensors: a systematic review. *IEEE Sensors Journal* 24:7375–7394

[18] Hixon DC. 1988. A guide to ion-selective electrodes. *Nature* 335:279–280

[19] Kumar V, Suri R, Mittal S. 2023. Review on new ionophore species for membrane ion selective electrodes. *Journal of the Iranian Chemical Society* 20:509–540

[20] Gao L, Tian Y, Gao W, Xu G. 2024. Recent Developments and Challenges in Solid-Contact Ion-Selective Electrodes. *Sensors* 24:4289

[21] Kunz W, Henle J, Ninham BW. 2004. 'Zur Lehre von der Wirkung der Salze' (about the science of the effect of salts): Franz Hofmeister's historical papers. *Current Opinion in Colloid & Interface Science* 9:19–37

[22] Reznicek J, Bednarik V, Filip J. 2023. Perchlorate sensing—Can electrochemistry meet the sensitivity of standard methods? *Electrochimica Acta* 445:142027

[23] Ertürün HEK, Özel AD, Ayanoğlu MN, Şahin Ö, Yılmaz M. 2017. A calix[4]arene derivative-doped perchlorate-selective membrane electrodes with/without multi-walled carbon nanotubes. *Ionics* 23:917–927

[24] Memon AA, Solangi AR, Memon S, Ali Bhatti A, Ali Bhatti A. 2015. Highly selective determination of perchlorate by a calix[4]arene based polymeric membrane electrode. *Polycyclic Aromatic Compounds* 36:106–119

[25] Ertürün HEK. 2017. Fabrication of a new carbon paste electrode based on 5,11,17,23-tetra-tert-butyl-25,27-bis(pyren-1-yl-methylimidopropoxy)-26,28-dihydroxy-calix[4]arene for potentiometric perchlorate determination. *International Journal of Electrochemical Science* 12:10737–10748

[26] Canel E, Erden S, Özel AD, Memon S, Yilmaz M, et al. 2008. A hydrogen ion-selective poly(vinyl chloride) membrane electrode based on calix[4]arene as a perchlorate ion-selective electrode. *Turkish Journal of Chemistry* 32:323–332

[27] Ganjali MR, Yousefi M, Poursaberi T, Naji L, Salavati-Niasari M, et al. 2003. Highly selective and sensitive perchlorate sensors based on some recently synthesized Ni(II)-hexaazacyclotetradecane complexes. *Electroanalysis* 15:1476–1480

[28] Ganjali MR, Norouzi P, Faridbod F, Yousefi M, Naji L, Salavati-Niasari M. 2007. Perchlorate-selective membrane sensors based on two nickel-hexaazamacrocycle complexes. *Sensors and Actuators B: Chemical* 120:494–499

[29] Rezaei B, Meghdadi S, Nafisi V. 2007. Fast response and selective perchlorate polymeric membrane electrode based on bis(dibenzoylmethanato) nickel(II) complex as a neutral carrier. *Sensors and Actuators B: Chemical* 121:600–605

[30] Soleymanpour A, Hamidi Asl E, Nabavizadeh SM. 2007. Perchlorate selective membrane electrodes based on synthesized platinum(II) complexes for low-level concentration measurements. *Sensors and Actuators B: Chemical* 120:447–454

[31] Soleymanpour A, Garaili B, Nabavizadeh SM. 2008. Perchlorate selective membrane electrodes based on a platinum complex. *Monatshefte Für Chemie - Chemical Monthly* 139:1439–1445

[32] Rezaei B, Meghdadi S, Bagherpour S. 2009. Perchlorate-selective polymeric membrane electrode based on bis(dibenzoylmethanato) cobalt(II) complex as a neutral carrier. *Journal of Hazardous Materials* 161:641–648

[33] Chandra S, Malik A, Tomar PK, Kumar A, Sadwal S. 2011. Perchlorate selective PVC membrane electrode based on Cobalt(II) complex of p-hydroxy acetophenone semicarbazone. *Analytical and Bioanalytical Electrochemistry* 3:379–392

[34] Gholamian F, Ali Sheikh-Mohseni M, Salavati-Niasari M. 2011. Highly selective determination of perchlorate by a novel potentiometric sensor based on a synthesized complex of copper. *Materials Science and Engineering: C* 31:1688–1691

[35] Onder A, Topcu C, Coldur F. 2018. Construction of a novel highly selective potentiometric perchlorate sensor based on neocuproine–Cu(II) complex formed in situ during the conditioning period. *Chemija* 29(1):57–66

[36] Gupta VK, Singh AK, Singh P, Upadhyay A. 2014. Electrochemical determination of perchlorate ion by polymeric membrane and coated graphite electrodes based on zinc complexes of macrocyclic ligands. *Sensors and Actuators B: Chemical* 199:201–209

[37] Sánchez-Pedreño C, Ortuño JA, Hernández J. 2000. Perchlorate-selective polymeric membrane electrode based on a gold(I) complex: application to water and urine analysis. *Analytica Chimica Acta* 415:159–164

[38] Hassan SSM, Galal Eldin A, Amr AEGE, Al-Omar MA, Kamel AH. 2019. Single-Walled Carbon Nanotubes (SWCNTs) as solid-contact in all-solid-state perchlorate ISEs: applications to fireworks and propellants analysis. *Sensors* 19:2697

[39] Shamsipur M, Soleymanpour A, Akhond M, Sharghi H, Hasaninejad AR. 2003. Perchlorate selective membrane electrodes based on a phosphorus(V)–tetraphenylporphyrin complex. *Sensors and Actuators B: Chemical* 89:9–14

[40] Casabó J, Escriche L, Pérez-Jiménez C, Muñoz JA, Teixidor F, et al. 1996. Application of a new phosphadithiamacrocycle to $ClO_4^-$-selective CHEMFET and ion-selective electrode devices. *Analytica Chimica Acta* 320:63–68

[41] Jain AK, Raisoni J, Kumar R, Jain S. 2007. Perchlorate selective sensor based on a newly synthesized hydrogen-bonding diamide receptor. *International Journal of Environmental Analytical Chemistry* 87:553–563

[42] Itterheimová P, Bobacka J, Šindelář V, Lubal P. 2022. Perchlorate Solid-Contact Ion-Selective Electrode Based on Dodecabenzylbambus[6]uril. *Chemosensors* 10

[43] Gil R, Amorim CG, Crombie L, Kong Thoo Lin P, Araújo A, et al. 2015. Study of a novel bisnaphthalimidopropyl polyamine as electroactive material for perchlorate-selective potentiometric sensors. *Electroanalysis* 27:2809–2819

[44] Errachid A, Pérez-Jiménez C, Casabó J, Escriche L, Munoz JA, et al. 1997. Perchlorate-selective MEMFETs and ISEs based on a new phosphadithiamacrocycle. *Sensors and Actuators B: Chemical* 43:206–210

[45] Joon NK, Barnsley JE, Ding R, Lee S, Latonen RM, et al. 2020. Silver(I)-selective electrodes based on rare earth element double-decker porphyrins. *Sensors and Actuators B: Chemical* 305:127311

[46] Bakker E, Pretsch E, Bühlmann P. 2000. Selectivity of potentiometric ion sensors. *Analytical Chemistry* 72:1127–1133

[47] Maccà C. 2004. Response time of ion-selective electrodes: Current usage versus IUPAC recommendations. *Analytica Chimica Acta* 512:183–190

[48] Ivanova NM, Levin MB, Mikhelson KN. 2012. Problems and prospects of solid contact ion-selective electrodes with ionophore-based membranes. *Russian Chemical Bulletin* 61:926–936

[49] Chaniotakis NA, Park SB, Meyerhoff ME. 1989. Salicylate-selective membrane electrode based on tin(IV)-tetraphenylporphyrin. *Analytical Chemistry* 61:566–570

[50] Cotton FA. 1999. *Advanced inorganic chemistry*. New York, Chichester: Wiley. 1355 pp.

[51] Gregory KP, Elliott GR, Robertson H, Kumar A, Wanless EJ, et al. 2022. Understanding specific ion effects and the Hofmeister series. *Physical Chemistry Chemical Physics* 24:12682–12718

[52] Grygolowicz-Pawlak E, Crespo GA, Ghahraman Afshar M, Mistlberger G, Bakker E. 2013. Potentiometric sensors with ion-exchange Donnan exclusion membranes. *Analytical Chemistry* 85:6208–6212

[53] Salvo-Comino C, Alonso-Pastor LE, Pérez-González C, Pettinelli S, Núñez Carrero KC, et al. 2025. Impact of molecular structure and plasticization of PVC membranes in the response of solid-state ion-selective electrodes. *Sensors and Actuators Reports* 9:100301

[54] Mahmoud H, Othmen K, Ncib S, Alyani I, Dammak L, et al. 2024. Effect of Plasticizer Type on Polymer Inclusion Membranes Properties and Performance for Zinc Separation. *ChemistrySelect* 9:e202303956

[55] Morawska K, Wardak C. 2024. Application of ionic liquids in ion-selective electrodes and reference electrodes: a review. *ChemPhysChem* 25:e202300818

[56] Mazloum Ardakani M, Jalayer M, Naeimi H, Zare HR, Moradi L. 2005. Perchlorate-selective membrane electrode based on a new complex of uranil. *Analytical and Bioanalytical Chemistry* 381:1186–1192

[57] Kozlowski C, Zawierucha I. 2025. Polymer Inclusion Membranes Based on Sulfonic Acid Derivatives as Ion Carriers for Selective Separation of Pb(II) Ions. *Membranes* 15:146

[58] Ocampo AL, Aguilar JC, Rodríguez de San Miguel E, Monroy M, Roquero P, et al. 2009. Novel proton-conducting polymer inclusion membranes. *Journal of Membrane Science* 326:382–387